Influence of Natural Organic Matter and Surface Charge on the Toxicity and Bioaccumulation of Functionalized Ceria Nanoparticles in Caenorhabditis elegans

ARTICLE *in* ENVIRONMENTAL SCIENCE & TECHNOLOGY · DECEMBER 2013

Impact Factor: 5.33 · DOI: 10.1021/es404503c · Source: PubMed

4 AUTHORS, INCLUDING:

Collin Blanche
Aix-Marseille Université
8 PUBLICATIONS **63** CITATIONS

SEE PROFILE

Olga Tsyusko
University of Kentucky
34 PUBLICATIONS **727** CITATIONS

SEE PROFILE

Environmental Science & Technology

Article

pubs.acs.org/est

Influence of Natural Organic Matter and Surface Charge on the Toxicity and Bioaccumulation of Functionalized Ceria Nanoparticles in *Caenorhabditis elegans*

Blanche Collin,* Emily Oostveen, Olga V. Tsyusko, and Jason M. Unrine*

University of Kentucky, Department of Plant and Soil Sciences, Lexington Kentucky 40546, United States

Supporting Information

ABSTRACT: The objective of this study was to investigate the role of the CeO_2 nanoparticle (NP) surface charge and the presence of natural organic matter (NOM) in determining bioavailability and toxicity to the model soil organism *Caenorhabditis elegans*. We synthesized CeO_2-NPs functionalized with positively charged, negatively charged, and neutral coatings. The positively charged CeO_2-NPs were significantly more toxic to *C. elegans* and bioaccumulated to a greater extent than the neutral and negatively charged CeO_2-NPs. Surface charge also affected the oxidation state of Ce in *C. elegans* tissues after uptake. Greater reduction of Ce from Ce (IV) to Ce (III) was found in *C. elegans*, when exposed to the neutral and negatively charged relative to positively charged CeO_2-NPs. The addition of humic acid (HA) to the exposure media significantly decreased the toxicity of CeO_2-NPs, and the ratio of CeO_2-NPs to HA influenced Ce bioaccumulation. When the concentration of HA was higher than the CeO_2-NP concentration, Ce bioaccumulation decreased. These results suggest that the nature of the pristine coatings as a determinant of hazard may be greatly reduced once CeO_2-NPs enter the environment and are coated with NOM.

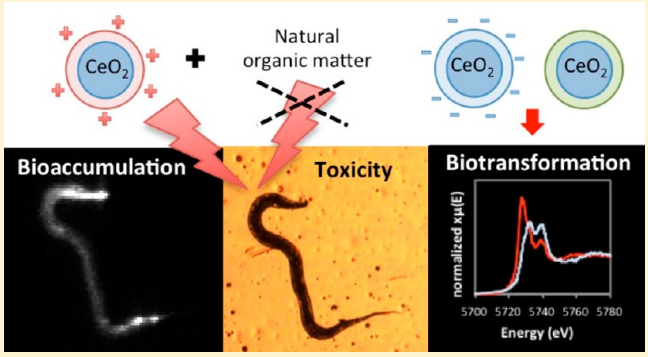

INTRODUCTION

Engineered nanomaterials are used in many commercial products and applications. Their production, use, and disposal will inevitably lead to environmental releases.[1,2] CeO_2 nanoparticles (CeO_2-NPs) are among the most important nanomaterials with increasing uses as polishing media,[3] catalysts in automotive fuel additives,[4] gas sensors, and other applications.[5] Ce in CeO_2-NPs can reversibly transition between Ce(III) and Ce(IV) valence states and can act as a regenerative catalyst due to oxygen vacancies present at the surface of the nanoparticles.[6] The magnitude of environmental releases of CeO_2-NPs and subsequent behavior and biological effects are currently unclear. The need for assessment of the environmental effects of these nanomaterials was expressed by international organizations such as the Organisation for Economic Cooperation and Development (OECD).[7] Given the limited number of ecotoxicological studies with CeO_2-NPs, the extent of their toxicity in the environment is uncertain. Toxicity in *Daphnia magna* and *Cophixalus riparius* has been reported at 1 mg L^{-1} after a 96 h exposure,[8] but in other studies no acute toxicity was measured in *D. magna* after the same duration exposure at 10 mg L^{-1} [9] or 48 h exposure at 1000 mg L^{-1}.[10] However, chronic exposures revealed higher toxicity in *D. magna*, with a threshold at 5.6 mg L^{-1} [10] and 100% mortality after 7 days at 10 mg L^{-1} CeO_2-NPs.[9]

There is evidence suggesting that CeO_2-NPs can act as a prooxidant or an antioxidant. Several investigations have reported that CeO_2-NP toxicity is caused by oxidative stress due to the reduction of Ce(IV) to Ce(III).[11,12] In direct contrast, CeO_2-NPs have also been found to possess biological antioxidant properties that can protect cells from damage caused by reactive oxygen species (ROS) both in vitro and in vivo.[13−15]

While CeO_2-NP size has been shown to influence reproduction and survival of *Caenorhabditis elegans*,[16] the toxic effects of the NPs can also be affected by their surface coating. The surface coating interfaces the NP with its biological environment and can control the pathways of cellular internalization. Therefore, toxicity can be influenced not only by the composition of the core but also by the coating.[17] For example, dextran coated CeO_2-NPs induced positive effects in in vivo studies, such as antitumor and antioxidant effects[18,19] while noncoated CeO_2-NPs induced toxicity.[12,20,21] Surface charge is another key property, which can control the colloidal stability of NP dispersion and transport in environmental and biological systems. In the context of in vitro studies, the surface charge of CeO_2-NPs has been shown to dictate NP subcellular localization in cells, and to influence their cytotoxicity.[22,23] Cationic NPs in general have been shown to be more toxic than their neutral or anionic counterparts.[24−26]

Received: October 8, 2013
Revised: December 13, 2013
Accepted: December 28, 2013
Published: December 29, 2013

An important aspect in risk assessment of manufactured nanomaterials is to understand their environmental interactions. The risks associated with exposure to NPs will be determined in part by the environmental processes that control NP fate, transport and transformation.[27] Exposure modeling has shown that soils are important sinks for engineered NPs.[1] Once in soils, NPs will interact with abundant organic ligands, including natural organic matter (NOM), which can result in the formation of a nanoscale coating on the NPs, changing their aggregation, sorption, and biological activity.[28,29] The vast majority of studies that have investigated how surface charge affects the toxicity of manufactured did not to take into account how these environmental transformations can impact the toxicity of pristine nanomaterials.

The objectives of this study were to investigate how charge of CeO_2-NP polymer coatings influences interaction with NOM and how this in turn affects particle stability and CeO_2-NP uptake, distribution, and toxicity to the model soil nematode *C. elegans*. Nematodes are important members of the terrestrial mesofauna, with a crucial role as grazers of microorganisms;[30] *C. elegans* have also been widely used as a model in aquatic/soil eco-toxicity testing of metals and NPs.[30−32]

We hypothesized that, due to its higher affinity with negatively charged biological membranes, CeO_2-NPs functionalized with a positively charged polymer would have increased toxicity and bioaccumulation in *C. elegans* compared to those functionalized with neutral or negatively charged polymers. We also hypothesized that toxicity of CeO_2-NPs in *C. elegans* will be associated with a reduction of Ce valence of IV to III. Finally, we hypothesized that the addition of NOM to positively charged CeO_2-NPs would decrease CeO_2-NP accumulation and toxicity in *C. elegans* by conferring a net negative surface charge over a wide pH range. We tested these hypotheses by exposing *C. elegans* to CeO_2-NPs of varying charge with or without NOM and measuring the effects on subsequent bioavailability and toxicity.

MATERIALS AND METHODS

Nanoparticle Synthesis and Characterization. Cerium dioxide NPs with 3 different stabilizing agents were investigated in this study. Dextran coated CeO_2-NPs with a nominal 4 nm primary particle diameter (DEX-CeO_2(0)) were synthesized using a modification of the procedure described by Perez et al.[18] This coating was then functionalized with diethylaminoethyl groups to confer either a net positive charge (diethylaminoethyl dextran; DEAE-CeO_2(+)), or carboxymethyl groups to confer a net negative charge (carboxymethyl dextran; CM-CeO_2(−)). Details of the synthesis and functionalization of the particles can be found in the Supporting Information (SI). Primary particle diameter was characterized by depositing the particles on carbon coated copper grids and examining with transmission electron microscopy (TEM; Jeol 2010F, Tokyo, Japan). Freeze-dried NPs and coatings were analyzed for functionalization on a Thermo-Fisher Nicolet 6700 Fourier transform infrared spectrometer. Electrophoretic mobility titrations were performed on each type of coated CeO_2-NP to gain insight into the intrinsic surface charge behavior imparted by the coatings as a function of pH in the exposure medium, which was moderately hard reconstituted water[33] (MHRW) (SI Figure S4). Mean hydrodynamic diameters and electrophoretic mobilities of the NP treatment suspensions were measured using a Nano-ZS zetasizer (Malvern Instruments, Malvern, United Kindgom), at a suspension concentration of 100 mg Ce L^{-1} CeO_2-NPs with and without 35 mg L^{-1} humic acid (HA), and 25 mg L^{-1} DEAE-CeO_2(+) in the presence of 0, 7, 35, 70 mg HA L^{-1} (SI Figures S6, S7, S8). Suspensions were prepared using the CeO_2-NP stock suspension and HA stock solution, adjusted at pH 8.1 and incubated at 25 °C for 24 h. The zeta potential was calculated using the Hückel approximation.

Pahokee Peat Humic Acid Solution. The soil humic acid Pahokee Peat (HA) obtained from the International Humic Substances Society (IHSS), was chosen as a soil HA model. HA was dissolved in 0.002N NaOH in DI (pH 7) at 500 mg HA L^{-1}. The HA solution was stirred overnight and filtered (cellulose acetate, 0.2 μm). This stock solution was kept at 4 °C. The total organic carbon measured in the stock solution, using a TOC-V_{CPN} total organic carbon analyzer (Shimadzu Corporation), was 182.6 mg C L^{-1}. According to the IHSS Pahokee peat HA is 52.12% C, therefore the actual concentration of the stock solution was 350 mg HA L^{-1}.

***Caenorhabditis elegans* Exposure.** *Caenorhabditis elegans* (wild type, Bristol strain N2) were obtained from the Caenorhabditis Genetics Center (Minneapolis, MN). The nematode culture maintenance, generation of age-synchronized worms and toxicity testing followed previously established protocols,[34] except the use of MHRW as exposure medium. MHRW was chosen in order to provide a chemical environment close to that found in soil pore water and for some ecological relevance. Mortality was measured after a 48 h of exposure at the L1 and L3 developmental stages. The exposure concentrations of DEAE-CeO_2(+) for L1 nematodes ranged from 0 to 100 mg Ce L^{-1} (0, 1, 5, 10, 25, 50, 75, and 100), while the exposure concentrations of the same NPs used for L3 animals ranged from 0 to 1000 mg Ce L^{-1} (0, 1, 5, 25, 100, 500, and 1000). A similar range of concentrations was also used for L1 nematodes exposed to DEX-CeO_2(0) and CM-CeO_2(-) (0, 100, 500, and 1000 mg Ce L^{-1}). All exposures for every concentration tested were conducted with and without 7 mg HA L^{-1}. As a control, the DEAE-DEX coating alone was tested at a concentration of 50 mg C L^{-1}, which would correspond to the concentration of C in a suspension of 200 mg Ce L^{-1} DEAE-CeO_2(+). *Escherichia coli* (strain OP50) was supplied as a food source (10 μg mL^{-1}, OD_{600} of 0.018) at the beginning and after 24 h of the exposure. All tests were conducted in 24-well polycarbonate tissue culture plates. Three replicates were performed for each test. A 1.0 mL aliquot of test solution was added to each well, which was subsequently loaded with 10 (±1) nematodes. The plates were observed under a stereomicroscope and the nematodes were counted and scored. Following an established protocol, nematodes that did not move in response to a gentle prod by a Pt wire were counted as dead.[35]

Synchrotron X-ray Analysis. In order to test the effect of CeO_2-NPs surface charge and the presence of HA on Ce bioaccumulation, *C. elegans* at the L3 stage were exposed to 100 mg Ce L^{-1} of DEX-CeO_2(0), CM-CeO_2(−) and DEAE-CeO_2(+) with and without 35 mg HA L^{-1} for 24 h without feeding. The presence of food (*E. coli*) in the media can affect NPs behavior and oxidation state.[12] We tested the effect of feeding on Ce bioaccumulation and speciation in *C. elegans* exposed to DEAE-CeO_2(+) for 24h with food (*E. coli* strain OP50). To further test the effects of HA on Ce accumulation and speciation, L3 stage *C. elegans* were exposed to 25 mg Ce L^{-1} DEAE-CeO_2(+) with 7, 35, and 70 mg HA L^{-1} for 48 h. We selected Ce concentrations that were below LC_{10} to ensure

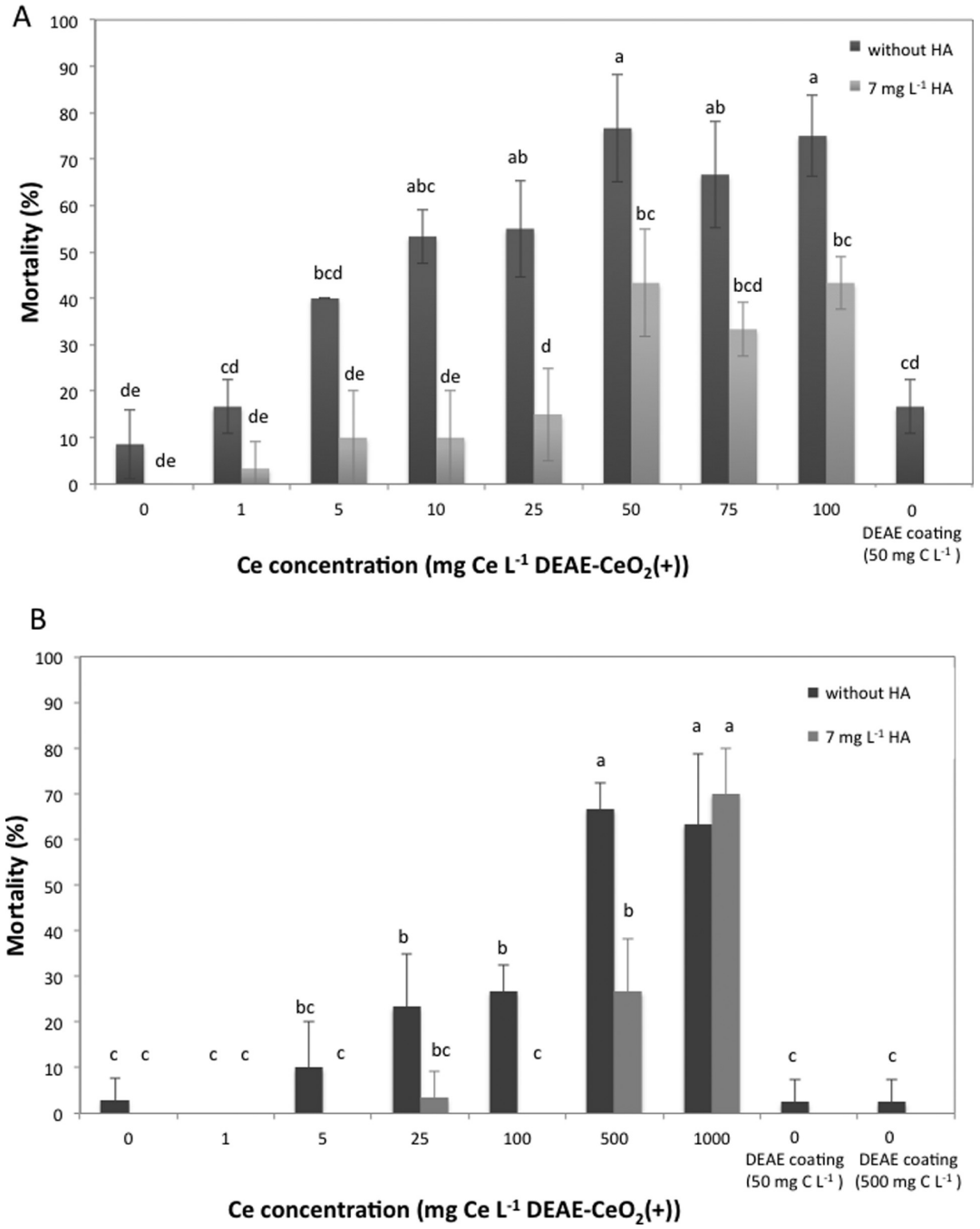

Figure 1. Mortality of *Caenorhabditis elegans* exposed to positively charged diethylaminoethyl-dextran coated CeO_2 nanoparticles (DEAE-CeO_2(+)) at L1 (A) and L3 (B) stages for 48 h with feeding. Diethylaminoethyl-dextran (DEAE) coating alone was also tested. Live *Escherichia coli*, strain OP50 bacteria were included as a nutrient source. Data are presented as the mean ± standard deviation (SD) (n = 3). Treatment labeled with the same letter did not differ significantly (Kruskal–Wallis test followed by pairwise Mann–Whitney U-tests, $p < 0.05$).

the nematode's survival during bioaccumulation experiment. After exposure, live nematodes were removed and preserved in 20% ethanol for up to a few days before X-ray analysis. The fresh samples were placed on metal-free polyimide film (Kapton; DuPont, Wilmington, DE) and immediately mounted in the X-ray beam. Several solutions were also prepared to analyze Ce speciation: NPs stock suspension, NPs in the MHRW, NPs after a 24h exposure, NPs with HA, and NPs with food (see SI Figure S10). Mixtures of 500 mg Ce L^{-1} CeO_2-NPs and 500 mg L^{-1} of ascorbic acid, tannic acid, albumin, glutathione, cysteine, collagen, and Na_2SO_4 (potential reductants) adjusted to pH 7 were also analyzed (SI Figure S11). These suspensions were analyzed in a cell constructed from polyimide tubing.

Scanning X-ray fluorescence microscopic measurements of Ce were collected at the Ce Lα_1 emission line (5750 eV) using beamline X-26A at the National Synchrotron Light Source at Brookhaven National Laboratory (Upton, NY). We used Ce L_{III}-edge X-ray absorption near-edge spectroscopy (XANES) to determine the oxidation state of Ce in CeO_2-NPs suspensions and on selected locations in *C. elegans* samples. Athena software was used to process the normalization and liner combination

fitting (LCF) of the XANES spectra.[36] *C. elegans* samples were fitted with 2 standards: Ce(III)sulfate as a Ce(III) standard and with the spectra of the NPs stock solution that they were exposed to, either DEX-CeO_2(0), CM-CeO_2(−), or DEAE-CeO_2(+), as a Ce(IV) standard. For every treatment, the proportions of Ce(III) and Ce(IV) obtained by LCF for each individual spectrum (SI Table S2) were averaged. Details of the analytical methods are provided in the SI.

Statistical Analyses. The SPSS statistic software package was used for statistical analyses. The data were tested for normality using the Shapiro-Wilk test and found to be non-normally distributed; therefore, we used nonparametric statistics. We tested for significant effects of treatments on Ce intensity, Ce speciation (proportion of Ce(III) or Ce(IV)) in *C. elegans*, and mortality using Kruskal−Wallis 1-way ANOVA followed by pairwise comparison using the Mann−Whitney U-test. Differences of $p < 0.05$ were considered statistically significant for all tests. Probit analysis was performed to calculate the median lethal concentration (LC_{50}) of *C. elegans* at L1 and L3 stages exposed to DEAE-CeO_2(+).

RESULTS AND DISCUSSION

Characterization of Nanoparticles. The TEM analysis showed the presence of NPs of similar core size (3.6−4) nm for all coatings (see SI Figure S1). The dextran functionalization was confirmed by the differences observed in the FTIR spectra: C−H stretching band at 2952 cm^{-1} for the DEAE-CeO_2(+) and several features characteristic of carboxylic acid for CM-CeO_2(−): C═O 1730 cm^{-1}, C−O 1320 cm^{-1}, and O−H 1400 cm^{-1} (SI Figure S2). On the basis of DLS data, we observed that the CeO_2-NPs in MHRW were monodisperse with volume weighted average hydrodynamic diameters of 13.9 nm, 17.8 and 15.3 nm for CM-CeO_2(−), DEX-CeO_2(0), and DEAE-CeO_2(+), respectively (SI Figure S3). Electrophoretic mobility measurements indicated that the DEX-CeO_2(0) have a point of zero net charge (PZC) in the vicinity of pH 6 (SI Figure S4) in MHRW. This value is lower than the reported value of a PZC at pH 8.1 for noncoated CeO_2-NPs in H_2O.[20,37] In the exposure media, the ζ potential (ZP) of DEAE-CeO_2(+), DEX-CeO_2(0), and CM-CeO_2(−) was +28.5, −9.3, and −31.5, respectively. From pH 4 to pH 9, CM-CeO_2(−) had a negative ZP and DEAE-CeO_2(+) had a positive ZP (SI Figure S4). Size measurements of DEX-CeO_2(0) were similar from pH 4 to 9 (SI Figure S5), which suggests that the NPs were sterically stabilized by the coating. Therefore, in the present study, *C. elegans* were tested with nonaggregated primary CeO_2-NPs, in contrast to most of the previous toxicity studies which used noncoated CeO_2-NPs, which strongly aggregated.[38−40]

The addition of HA to the suspension did not significantly modify the hydrodynamic diameter of CM-CeO_2(−) or DEX-CeO_2(0) (SI Table S1). However, the hydrodynamic diameter and the surface charge of the DEAE-CeO_2(+) were strongly affected by the presence of HA. The addition of 35 mg HA L^{-1} to a 100 mg Ce L^{-1} DEAE-CeO_2(+) suspension only shifted the ZP slightly, from +28.5 mV to +21.9 mV, but it did induce the aggregation of the NPs (SI Figure S6). Pahokee Peat HA in solution had a single peak centered at 18.2 nm (SI Figure S6) and a ZP of −41 mV. For a 25 mg Ce L^{-1} DEAE-CeO_2(+) suspension, the addition of 7 mg HA L^{-1} only slightly decreased the positive ZP while 35 mg L^{-1} and 70 mg HA L^{-1} induced a negative ZP (−12.4 mV and −30 mV, respectively) (SI Figure S7). For 7 mg HA L^{-1}, the majority of the NPs were not aggregated and were similar in size to unaltered DEAE-CeO_2(+), but two other small peaks appeared at 40 and 5000 nm. A 35 mg HA L^{-1} concentration induced the formation of larger aggregates having hydrodynamic sizes of ∼5000 nm (SI Figure S8). The formation of aggregates may be explained through the bridging of the negatively charged HA to anionic functional groups of DEAE-CeO_2(+). Bridging via Ca^{2+} complexation,[41,42] present in MHRW, may also be involved but not as the main mechanism, since aggregation was also observed in pure water. With an increase of HA concentration to 70 mg L^{-1}, the aggregates were smaller with two principal size fractions: one ranging from 30 to 200 nm and another around 5000 nm (SI Figure S8). The increase of negative charge and HA adsorption could enhance both electrostatic and steric repulsion between NPs, therefore reducing the aggregation.[43] Thereby, the presence of HA in the suspensions induced the formation of agglomerates but their charges, sizes, and stabilities in suspensions were dependent on the ratio between DEAE-CeO_2(+) and HA concentrations.

Toxicity Testing. CeO_2-NPs with negatively charged or neutral coatings had very low toxicity for the end point measured in contrast with positively charged coating. After a 48 h exposure of L1 stage *C. elegans* to 1000 mg Ce L^{-1} DEX-CeO_2(0) or CM-CeO_2(−), only 16.7% and 3.3% mortality was measured, respectively (see SI Figure S12). However, mortality of *C. elegans* significantly increased over the range of 1−50 mg Ce L^{-1} DEAE-CeO_2(+) and then plateaued at about 75% (Figure 1). For instance, a 48 h exposure of L1 stage *C. elegans* to 50 mg Ce L^{-1} DEAE-CeO_2(+) induced 76% mortality. The extent of toxicity depended on the developmental stage of the nematodes: L3 stage *C. elegans* were more resistant than younger L1 stage with LC_{50} of 272 and 15.5 mg Ce L^{-1} for L3 and L1, respectively. The DEAE-DEX coating alone at 50 mg C L^{-1}, which would be the coating concentration in a suspension of 200 mg Ce L^{-1} DEAE-CeO_2(+), induced only 2.5% for L3 and 16.7% mortality for L1, which was not statistically different from the control (Mann−Whitney U-test, $p = 0.429$) (Figure 1). An even higher coating concentration at 500 mg C L^{-1} tested at the L3 stage did not induce any toxicity (Figure 1). Therefore, the coating itself does not explain the high toxicity measured for DEAE-CeO_2(+). Dextran coated CeO_2-NPs have been shown to be relatively nontoxic in vitro when exposed to normal cells, cardiac myocytes, human embryonic kidney and cancer cells, lung and breast carcinomas,[22] and in vivo to *E. coli* under a wile range of experimental conditions.[48] However, our results contrast with the cytotoxicity study of Yang et al.[49] in which DEX coated CeO_2-NPs (−5 mV) and positively charged DEX-*N*,*N*-dimethylethylenediamine-CeO_2-NPs (+32 mV) did not induce a significant cytotoxicity in cell lines of human colorectal adenocarcinoma, lung carcinoma and ovarian adenocarcinoma up to 120 mg Ce L^{-1} regardless of the surface charge.

Previous studies of *C. elegans* demonstrated effects of noncoated CeO_2-NPs on growth and reproduction[16,39] at 2.5 and 1 mg L^{-1} respectively, similar to those that we used to examine mortality after exposure of L1 stage *C. elegans* to DEAE-CeO_2(+). Zhang et al.[11] observed the effects on *C. elegans* life span at very low concentrations such as 1 nM (172 ng L^{-1}). Since different end points, exposure conditions, exposure media and different NP coatings were used in these studies, we cannot directly compare results. For instance, Zhang et al.[11] used an unusual coating, hexamethyleneteramine. In the present study, we demonstrated that the coatings alone did not

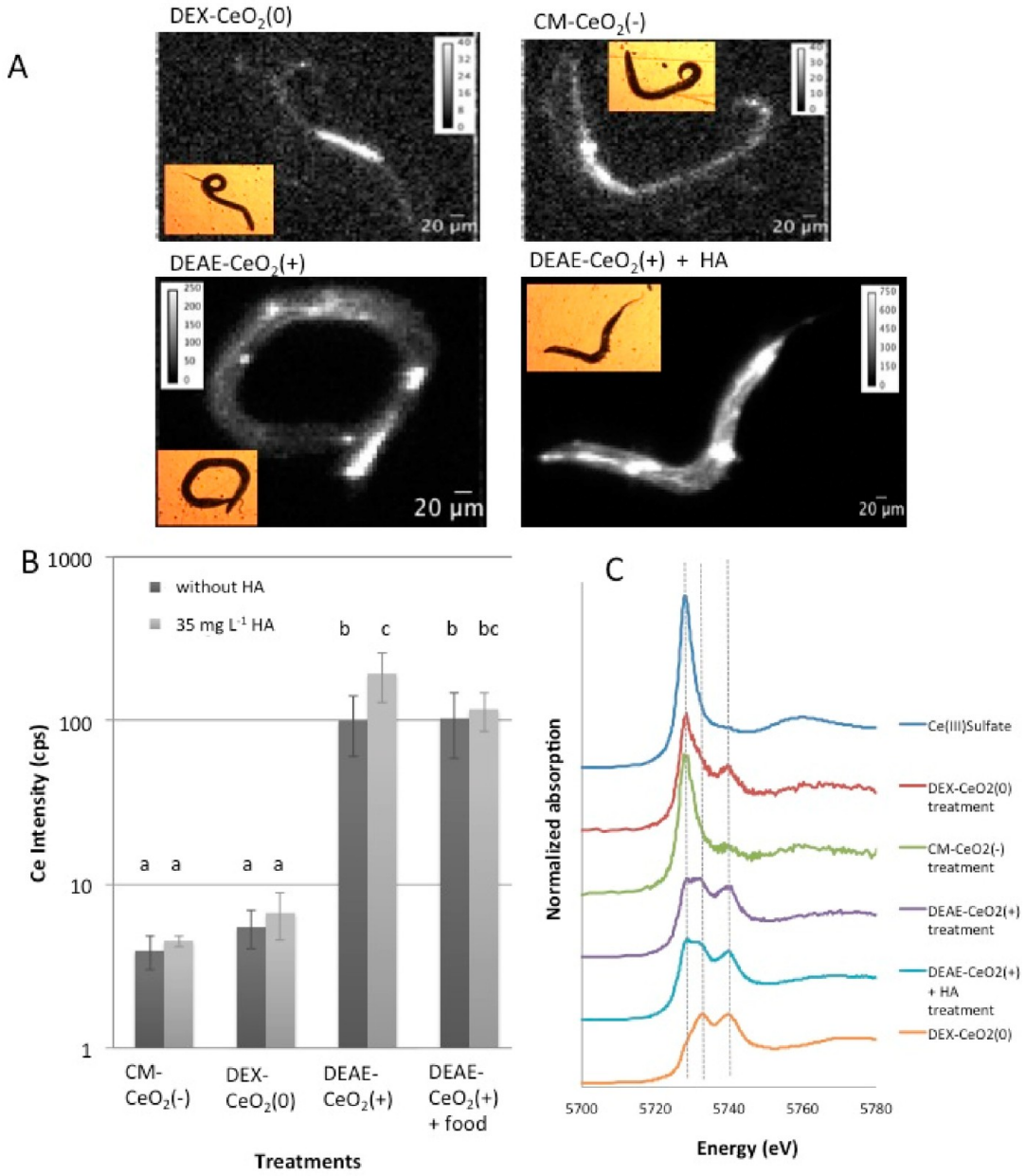

Figure 2. (A) X-ray fluorescence microprobe (μXRF) maps of the Ce L-α edge, and light micrographs of *Caenorhabditis elegans* (*C. elegans*) exposed at stage L3 for 24 h to 100 mg Ce L^{-1} carboxymethyl-dextran coated CeO_2 nanoparticles (CM-CeO_2(−)), 100 mg Ce L^{-1} dextran coated CeO_2 nanoparticles (DEX-CeO_2(0)), 100 mg Ce L^{-1} diethylaminoethyl-dextran coated CeO_2 nanoparticles (DEAE-CeO_2(+)), 100 mg Ce L^{-1} DEAE-CeO_2(+) and 35 mg L^{-1} humic acid (HA). (B) Ce intensity (counts per seconds [cps]) measured on *C. elegans* at Ce L-α edge. *C. elegans* were exposed to 100 mg Ce L^{-1} CeO_2-NPs with and without 35 mg HA L^{-1}. In the treatment "DEAE+food" *Escherichia coli* (strain OP50) was added as food. Data are presented as the mean ± standard deviation (SD) ($5 \leq n \leq 15$). Treatment labeled with the same letter did not differ significantly (Kruskal−Wallis test followed by pairwise Mann−Whitney *U*-tests, $p < 0.05$). (C) Typical XANES spectra measured on a hot spot of *C. elegans* specimens from the same treatments and two reference spectra, Ce(III)sulfate and DEX-CeO_2(0).

explain the measured toxicity in *C. elegans*, but this has not been shown for hexamethyleneteramine.[11]

Influence of Surface Charge on Ce Accumulation and Ce Speciation. Figure 2A shows an optical micrograph and the μ-XRF Ce intensity map of *C. elegans* exposed to 100 mg Ce L^{-1} of DEX-CeO_2(0), CM-CeO_2(−), DEAE-CeO_2(+), and 100 mg Ce L^{-1} DEAE-CeO_2(+) and 35 mg HA L^{-1} for 24 h. Ce accumulated in *C. elegans* tissues for all treatments but the Ce intensity was significantly lower for DEX-CeO_2(0) and CM-CeO_2(−) treatments than for DEAE-CeO_2(+) (Mann−Whitney U-test, $p = 0.007$ and $p = 0.001$, respectively) (Figure 2B). *C. elegans* exposed to DEAE-CeO_2(+) accumulated 25 and 20 times more Ce than *C. elegans* exposed to DEX-CeO_2(0) and CM-CeO_2(−), respectively. Therefore, the surface charge had a strong effect on Ce bioaccumulation. DEAE-CeO_2(+) induced greater toxicity combined with a greater Ce accumulation in *C. elegans* than the neutral and negatively charged DEX-CeO_2(0) and CM-CeO_2(−), respectively. The presence of food (*E. coli* strain OP50) did not modify the Ce bioaccumulation to *C. elegans* exposed to DEAE-CeO_2(+) (Figure 2B).

dx.doi.org/10.1021/es404503c | *Environ. Sci. Technol.* 2014, 48, 1280−1289

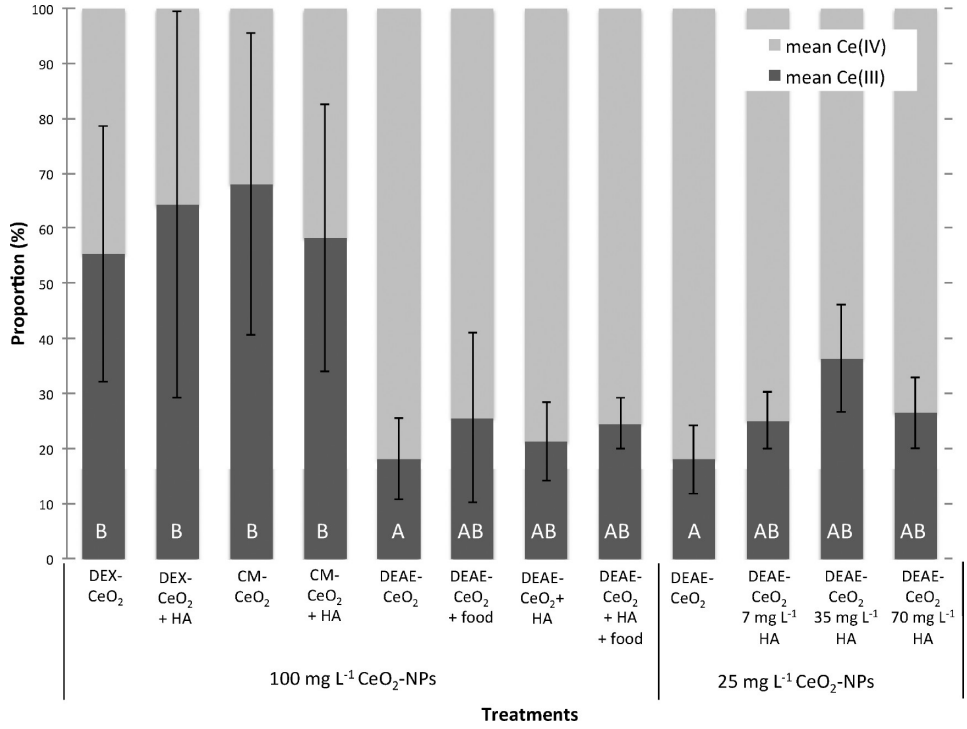

Figure 3. Proportions of Ce ligands having Ce in a reduced form [Ce(III)] or oxidized form [Ce(IV)] as determined by linear combination fitting of the *Caenorhabditis elegans* specimens normalized Ce L_{III}-edge X-ray absorption near-edge spectroscopy (XANES). Data are presented as the mean ± standard deviation (SD) ($6 \leq n \leq 9$). Treatment labeled with the same letter did not differ significantly (Kruskal–Wallis test followed by pairwise Mann–Whitney *U*-tests, $p < 0.05$).

The *C. elegans* normalized Ce L_{III}-edge XANES spectra were compared to Ce(III) standard and CeO_2 NPs spectrum (Figure 2C). Pronounced differences can be observed in XANES spectra between a Ce(III) compound and a Ce(IV) compounds (see SI Figure S9). For Ce(III) atoms, a dominant single post absorption edge peak ("white line") is observed at 5729 eV. For Ce(IV), the major band exhibited a double white line characteristic of a mixture of two Ce ground-state electronic configurations, $4f^0L$ and $4f^1L$.[44] The CeO_2-NP spectra are in good agreement with the CeO_2–Ce(IV) reference spectra (SI Figure S9), which is also observed in other studies.[12,46] XANES spectra of DEX-CeO_2(0), CM-CeO_2(−), and DEAE-CeO_2(+) were all similar (SI Figure S9). Therefore, the coating and functionalization procedure had no influence on the Ce speciation of the NPs. CeO_2-NPs incubated with various inorganic and organic compounds, in MHRW or with different NOM, presented the same speciation as CeO_2-NPs in MHRW water (SI Figures S10 and S11). Therefore, these results provide evidence that the CeO_2-NPs were not modified in the exposure media. Similarly, no reduction of Ce(IV) was measured on CeO_2-NPs that interacted with macromolecules IgG and BSA.[47] The *C. elegans* Ce L_{III}-edge XANES spectra exhibited peaks corresponding to both Ce(III) and Ce(IV) for all CeO_2-NPs treatments Figure 2C. Therefore, Ce(IV) from CeO_2-NPs was partially reduced to Ce(III) in *C. elegans*. The LCF results showed that the majority of Ce in *C. elegans* exposed to DEX-CeO_2(0) and CM-CeO_2(−) was present as Ce(III) (68.1 ± 27.4% and 55.3 ± 23.2%, respectively), whereas *C. elegans* exposed to DEAE-CeO_2(+) had only 18 ± 7.4% Ce(III) (Figure 3). Nanoparticles were also analyzed by XANES in exposure media collected after *C. elegans* exposures (see SI Figure S10). The CeO_2-NPs in the exposure media remained unaltered.

The results suggest that the adsorption and/or internalization of CeO_2-NPs in *C. elegans*, regardless of surface charge, affected the redox state of CeO_2-NPs. The reduction of Ce(IV) to Ce(III) in CeO_2-NPs has been observed during the contact between CeO_2-NPs and *E. coli*,[12] cucumber plants,[50] and to a lesser extent, soybean.[46] The Ce reduction may explain the toxicity induced by these NPs by suggesting oxidative damage of macromolecules or generation of ROS. However, the fact that *C. elegans* exposed to the less toxic NPs (CM-CeO_2(−) and DEX-CeO_2(0)) had a higher proportion of reduced Ce compared to the nematodes exposed to DEAE-CeO_2(+) is surprising. Several hypotheses may be proposed to explain it:

(i) Given the low Ce bioaccumulation in *C. elegans* exposed to DEX-CeO_2(0) or CM-CeO_2(−), the nematodes may be able to cope with the oxidative stress induced by Ce. Indeed, even though the proportion of Ce(III) is higher in *C. elegans* exposed to CM-CeO_2(−) or DEX-CeO_2(0) compared to DEAE-CeO_2(+), due to the higher quantity of Ce accumulated, the Ce(III) concentration was 6.6 times higher in DEAE-CeO_2(+) than in CM-CeO_2(−) and DEX-CeO_2(0) exposed nematodes (SI Figure S13).

(ii) A portion of Ce in CM-CeO_2(−) and DEX-CeO_2(0) may have been dissolved in the exposure media or in *C. elegans* tissues. In the media, no dissolved Ce was measured (<0.42 μg Ce L^{-1}) in DEX-CeO_2(0), CM-CeO_2(−) and DEAE-CeO_2(+) suspensions and after a 24 h-exposure to *C. elegans* (see SI Table S2). So the Ce(III) absorption by the nematodes seems negligible. CeO_2 is not necessarily subject to reductive dissolution since Ce_2O_3 is also relatively insoluble.[51] The acidic pH of the pharyngeal and intestinal lumen of *C. elegans*, which ranges from 5.96 to 3.59,[53] may favor dissolution.[52] However, extensive dissolution in the gut

dx.doi.org/10.1021/es404503c | *Environ. Sci. Technol.* 2014, 48, 1280–1289

and in the cellular environment seems unlikely. For example, a recent study in rats demonstrated that there was no clearance of 5−55 nm CeO_2-NPs over 720 h, which would be unexpected if significant dissolution occurred. This study also demonstrated that the CeO_2-NPs remained intact within tissues leading to granuloma formation.[55] However, in a study of cucumber plants there is some evidence that a relatively small amount (not quantified) of Ce dissolved and precipitated as $CePO_4$ in roots due to release of root exudates and high concentrations of phosphate in the nutrient media.[50] Unfortunately, the XANES spectra for most Ce(III) compounds are nearly identical, making identification beyond oxidation state difficult. For example, the two Ce(III) standards ($CePO_4$ and $Ce(CH_3COO)_3$) had identical XANES spectra in their study. Also, dissolved Ce(III) was not measured in the hydroponic solution.

(iii) NP surface charge may have modified their internalization and localization both in tissue and in cells. At the cellular level, different cellular compartments have different redox characteristics,[56] so the local environment of the NPs may influence their reactivity and therefore Ce reduction. The negative membrane potential of most cells interacts differently with particles with a positive or negative surface charge.[57,58] The electrostatic interaction of NPs with the negatively charged bilayer of a membrane has been shown to mediate their binding[59] and their toxicity.[26,60] Higher cytotoxicity potential of positively charged NPs has been predominantly related to higher cellular uptake.[26,57] One common effect of a direct interaction of cationic NPs with cells is their ability to disrupt a cell membrane's lipid bilayer.[61] Upon internalization, the surface functionality of NPs dictates their behavior. Asati et al.[22] showed that negatively charged CeO_2-NPs were primarily localized in the cytoplasm, whereas positively charged CeO_2-NPs were localized preferentially in the lysosomes and became toxic due to acidic microenvironment of these organelles, which activated the oxidase activity of CeO_2-NPs.

Beyond the cellular level, NP accumulation in tissues and organs also depends on NP surface properties.[62,63] We can observe on the μ-XRF Ce images that CM-CeO_2(−) and DEX-CeO_2(0) seem to be mainly accumulated in the gut, while DEAE-CeO_2(+) was not only detected in the gut but throughout the nematode body (Figure 2A). In addition to the negatively charged lipid bilayer of cells, the *C. elegans* cuticle is covered by the glycoprotein-rich negatively charged surface coat.[64] Electrostatic attraction between the cuticle and the positively charged DEAE-CeO_2(+) may have also enhanced adsorption.

Influence of Humic Acid. The addition of 7 mg HA L^{-1} significantly decreased toxicity for DEAE-CeO_2(+) at concentrations up to 500 mg Ce L^{-1}, for both the L1 and L3 larval stages (Figure 1). Mortalities due to DEX-CeO_2(0) and CM-CeO_2(−) were not modified by the addition of HA and were lower than 6.7% up to 1000 mg Ce L^{-1} with 7 mg HA L^{-1} (SI Figure S12). This is not surprising, given the relative lack of toxicity of the pristine particles. Ce accumulation, measured by μ-XRF (Figure 2B) in *C. elegans* exposed for 24 h to 100 mg Ce L^{-1} CM-CeO_2(−) and DEX-CeO_2(0) was similar with or without the addition of 35 mg HA L^{-1}. On the other hand, the average intensity of Ce accumulated in *C. elegans* exposed to 35 mg HA L^{-1} and 100 mg Ce L^{-1} DEAE-CeO_2(+) was 194 ± 65 counts per second (cps), whereas without HA, the intensity was 100 ± 40 cps. Therefore, HA addition induced a significant increase of Ce bioaccumulation for the DEAE treatment. The higher Ce accumulation in the presence of HA may be explained by the absorption of CeO_2-NPs and HA agglomerates. During the exposure, the larger agglomerates (>2 μm) (SI Figure S6) may have settled onto the bottom of the well plates, locally increasing the Ce exposure concentration to *C. elegans*, which typically dwell near the bottom of the wells. The addition of *E. coli* did not modify the Ce accumulated by *C. elegans* exposed to DEAE-CeO_2(+) without HA but decreased the Ce accumulated by *C. elegans* exposed to HA and DEAE-CeO_2(+) compared to the same treatment without food (Figure 2). This may indicate that in the absence of food, the nematodes were filter feeding on the CeO_2 and HA aggregates, which led to a higher rate of ingestion and subsequent assimilation.

The Ce oxidation state in animals exposed to 100 mg Ce L^{-1} DEAE-CeO_2(+) was not significantly affected by the presence of HA or food, with a high proportion of Ce measured as Ce(IV): from 73 to 82% (Figure 3).

Addition of 7 mg HA L^{-1} to 25 mg Ce L^{-1} DEAE-CeO_2(+) significantly increased Ce intensity measured in *C. elegans* from an average of 47.8 ± 15 to 77 ± 18 cps (Figure 4). The addition of 35 mg HA L^{-1} induced a wide variation of Ce intensity, varying between 15.5 and 247 cps, with an average at 139 ± 108 cps. The addition of 70 mg HA L^{-1} concentration significantly decreased the Ce accumulation compared to other treatments, reaching 9.5 ± 4.5 cps. The higher Ce bioaccumulation with 7 mg HA L^{-1} compared to that without HA may be partly explained by the absorption of small aggregates. At these HA and NPs concentrations, most of the aggregates had an average size of 11.7 nm, but two larger size fractions were formed at 40 nm and >2 μm (SI Figure S8). For the 35 mg HA L^{-1} treatment, the presence of μm size aggregates (SI Figure S8) explained this important variability. As we can observe on the μ-XRF map of this treatment (Figure 4), some aggregates can adhere to the nematode cuticle and drastically influence the Ce intensity. The samples (2 out of 5) where no aggregates were observed on the nematode had a lower Ce intensity than the control. This seems to indicate that the actual absorbed concentrations were lower. Moreover, most of the aggregates were too large to be absorbed by *C. elegans*. As a filter-feeder, its pharynx and buccal cavity exclude larger particles than 3 μm in young adults.[65] The large size of aggregates may also partly explain the significant decrease of Ce accumulation in *C. elegans* in the 70 mg HA L^{-1} treatment. But for smaller aggregates, the low accumulation may be mainly explained by the change in ZP, which became negative.

These results showed that the presence of HA greatly influenced Ce accumulation in *C. elegans*, increasing its accumulation for a high NP/HA ratio, and decreasing it for a low NP/HA ratio. Therefore, while the toxicity was always decreased in the presence of HA, Ce bioaccumulation is highly dependent on the ratio of NPs to HA. In all specimens exposed to 25 mg Ce L^{-1} DEAE-CeO_2(+), Ce was mainly present as Ce(IV), with a proportion ranging from 19.3% without HA to 38% with 50 mg HA L^{-1} (Figure 3). The high Ce accumulation coupled with a low toxicity in *C. elegans* exposed to a high NP/HA ratio showed that the presence of HA reduced the inherent toxicity of DEAE-CeO_2(+). Several processes can explain how HA could have alleviated toxicity despite increased bioaccumulation. The adsorption of HA at the surface of the NPs can

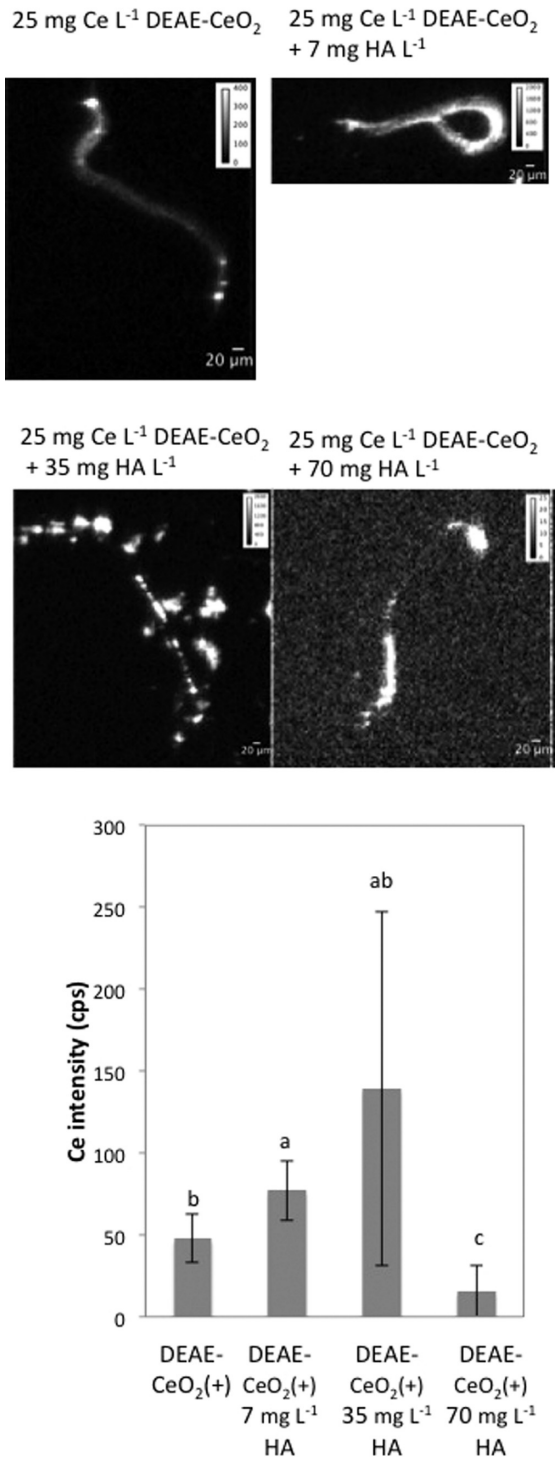

Figure 4. X-ray fluorescence microprobe (μXRF) maps of the Ce L-α edge of *Caenorhabditis elegans* specimens (stage L3) that were exposed for 48h to 25 mg Ce L^{-1} of positively charged diethylaminoethyl-dextran coated CeO_2 nanoparticles (DEAE-CeO_2(+)) and 7, 35, or 70 mg L^{-1} humic acid (HA). Data are presented as the mean ± standard deviation (SD) ($5 \leq n \leq 7$). Treatment labeled with the same letter did not differ significantly (Kruskal–Wallis test followed by pairwise Mann–Whitney *U*-tests, $p < 0.05$).

form a physical barrier to NP interaction with the cell membrane and also reduce binding of NPs to important proteins and biomolecules.[8,66] In another study, aqueous organic matter may have also mitigated nC60 toxicity by coating the NPs, hindering direct contact with the cells and possibly altering nC60 surface chemistry through an undetermined mechanism.[67] It is possible that in our study, the partial HA adsorption was sufficient to decrease the toxicity by reducing the reactivity between cells and CeO_2-NP surfaces, but not to reverse the zeta potential so it did not decrease the NP absorption. The HA may also act as an antioxidant by reacting with ROS,[66,68] which would mitigate the oxidative stress of CeO_2-NPs. These effects cannot be confirmed in this study as no significant decrease in the amount of reduced Ce in *C. elegans* was measured with HA (Figure 3). However, HA may have intercepted reactive oxygen species that were generated without affecting the overall valence of the particles.

Environmental Implications. This study showed that the surface chemistry of pristine CeO_2-NPs, specifically their charge, had a profound effect on their toxicity. The positively charged DEAE-CeO_2(+) were far more toxic to *C. elegans* and were bioaccumulated to a greater extent than the neutral and negatively charged DEX-CeO_2(0) and CM-CeO_2(−). Surface charge also influenced the oxidation state of CeO_2-NPs once taken up by *C. elegans*. The addition of HA to the exposure medium decreased the toxicity of CeO_2-NPs, and its concentration was shown to influence Ce bioaccumulation. For a higher ratio of HA to NPs, which is a more relevant scenario in the environment, the presence of HA significantly decreased Ce bioaccumulation. This work suggests that although initial surface chemistry had a profound impact on toxicity, environmental transformations (specifically coating with natural organic matter) reduced the effects of initial surface chemistry, and rendered ultrasmall (2–5 nm), positively charged CeO_2-NPs significantly less toxic for the end points tested at environmentally realistic ratios of HA to CeO_2.

■ ASSOCIATED CONTENT

Ⓢ Supporting Information

Additional data on nanoparticle characterization, μ-XANES analysis, and *C. elegans* toxicity. This material is available free of charge via the Internet at http://pubs.acs.org.

■ AUTHOR INFORMATION

Corresponding Author

*Phone: (859)-257-2467; e-mail: Jason.Unrine@uky.edu (J.M.U.), Blanche.Collin@uky.edu (B.C.).

Notes

The authors declare no competing financial interest.

■ ACKNOWLEDGMENTS

This research was supported by the United States Environmental Protection Agency (U.S. EPA) through a Science to Achieve Results (STAR) grant (RD-83485701-0). J.M.U. and O.T. were supported by the National Science Foundation (NSF) through cooperative agreement EF-0830093 (Center for Environmental Implications of Nanotechnology). It has not been formally reviewed by EPA or NSF. The views expressed in this document are solely those of the authors. EPA and NSF do not endorse any products or commercial services mentioned in this publication. Portions of this work were performed at Beamline X26A, National Synchrotron Light Source (NSLS), Brookhaven National Laboratory. X26A is supported by the Department of Energy (DOE)–Geosciences (DE-FG02-92ER14244 to The University of Chicago–CARS). Use of the NSLS was supported by DOE under Contract No. DE-

AC02-98CH10886. The authors gratefully acknowledge W. Rao, S. Wirick, D. McNear, J. Kupper, J. Nelson, P. Bertsch, A. Butterfield, U. Graham, S. Rathnayake, and S. Shrestha.

REFERENCES

(1) Gottschalk, F.; Nowack, B. The release of engineered nanomaterials to the environment. *J. Environ. Monit.* **2011**, *13* (5), 1145−55.

(2) Klaine, S. J.; Alvarez, P. J. J.; Batley, G. E.; Fernandes, T. F.; Handy, R. D.; Lyon, D. Y.; Mahendra, S.; McLaughlin, M. J.; Lead, J. R. Nanomaterials in the environment: Behavior, fate, bioavailability, and effects. *Environ. Toxicol. Chem.* **2008**, *27* (9), 1825−1851.

(3) Yu, T.; Park, Y. I.; Kang, M. C.; Joo, J.; Park, J. K.; Won, H. Y.; Kim, J. J.; Hyeon, T. Large-scale synthesis of water dispersible ceria nanocrystals by a simple sol-gel process and their use as a chemical mechanical planarization slurry. *Eur. J. Inorg. Chem.* **2008**, *6*, 855−858.

(4) Park, B.; Donaldson, K.; Duffin, R.; Tran, L.; Kelly, F.; Mudway, I.; Morin, J. P.; Guest, R.; Jenkinson, P.; Samaras, Z.; Giannouli, M.; Kouridis, H.; Martin, P. Hazard and risk assessment of a nanoparticulate cerium oxide-based diesel fuel additive - a case study. *Inhal. Toxicol.* **2008**, *20* (6), 547−66.

(5) Trovarelli, A.; de Leitenburg, C.; Boaro, M.; Dolcetti, G. The utilization of ceria in industrial catalysis. *Catal. Today* **1999**, *50* (2), 353−367.

(6) Heckert, E. G.; Karakoti, A. S.; Seal, S.; Self, W. T. The role of cerium redox state in the SOD mimetic activity of nanoceria. *Biomaterials* **2008**, *29* (18), 2705−2709.

(7) OECD. List of manufactured nanomaterials and list of endpoints for phase one of the OECD testing programme. In *Series on the Safety of Manufactured Nanomaterials No. 6*; Organization for Economic Cooperation and Development: Paris, France, 2008.

(8) Lee, S. W.; Kim, S. M.; Choi, J. Genotoxicity and ecotoxicity assays using the freshwater crustacean *Daphnia magna* and the larva of the aquatic midge *Chironomus riparius* to screen the ecological risks of nanoparticle exposure. *Environ. Toxicol. Pharmacol.* **2009**, *28* (1), 86−91.

(9) Gaiser, B. K.; Biswas, A.; Rosenkranz, P.; Jepson, M. A.; Lead, J. R.; Stone, V.; Tyler, C. R.; Fernandes, T. F. Effects of silver and cerium dioxide micro- and nano-sized particles on *Daphnia magna*. *J. Environ. Monit.* **2011**, *13*, (5).

(10) Van Hoecke, K.; Quik, J. T. K.; Mankiewicz-Boczek, J.; De Schamphelaere, K. A. C.; Elsaesser, A.; Van der Meeren, P.; Barnes, C.; McKerr, G.; Howard, C. V.; Van De Meent, D.; Rydzynski, K.; Dawson, K. A.; Salvati, A.; Lesniak, A.; Lynch, I.; Silversmit, G.; De Samber, B.; Vincze, L.; Janssen, C. R. Fate and effects of CeO_2 nanoparticles in aquatic ecotoxicity tests. *Environ. Sci. Technol.* **2009**, *43* (12), 4537−4546.

(11) Zhang, H.; He, X.; Zhang, Z.; Zhang, P.; Li, Y.; Ma, Y.; Kuang, Y.; Zhao, Y.; Chai, Z. Nano-CeO_2 exhibits adverse effects at environmental relevant concentrations. *Environ. Sci. Technol.* **2011**, *45* (8), 3725−3730.

(12) Thill, A.; Zeyons, O.; Spalla, O.; Chauvat, F.; Rose, J.; Auffan, M.; Flank, A. M. Cytotoxicity of CeO_2 nanoparticles for *Escherichia coli*. Physico-chemical insight of the cytotoxicity mechanism. *Environ. Sci. Technol.* **2006**, *40* (19), 6151−6156.

(13) Celardo, I.; Pedersen, J. Z.; Traversa, E.; Ghibelli, L. Pharmacological potential of cerium oxide nanoparticles. *Nanoscale* **2011**, *3* (4), 1411−1420.

(14) Xia, T.; Kovochich, M.; Liong, M.; Madler, L.; Gilbert, B.; Shi, H.; Yeh, J. I.; Zink, J. I.; Nel, A. E. Comparison of the mechanism of toxicity of zinc oxide and cerium oxide nanoparticles based on dissolution and oxidative stress properties. *ACS Nano* **2008**, *2* (10), 2121−34.

(15) Karakoti, A. S.; Munusamy, P.; Hostetler, K.; Kodali, V.; Kuchibhatla, S.; Orr, G.; Pounds, J. G.; Teeguarden, J. G.; Thrall, B. D.; Baer, D. R. Preparation and characterization challenges to understanding environmental and biological impacts of ceria nanoparticles. *Surf. Interface Anal.* **2012**, *44* (8), 882−889.

(16) Roh, J. Y.; Park, Y. K.; Park, K.; Choi, J. Ecotoxicological investigation of CeO_2 and TiO_2 nanoparticles on the soil nematode *Caenorhabditis elegans* using gene expression, growth, fertility, and survival as endpoints. *Environ. Toxicol. Pharmacol.* **2010**, *29* (2), 167−172.

(17) Rivera-Gil, P.; De Aberasturi, D. J.; Wulf, V.; Pelaz, B.; Del Pino, P.; Zhao, Y. Y.; De La Fuente, J. M.; De Larramendi, I. R.; Rojo, T.; Liang, X. J.; Parak, W. J. The challenge to relate the physicochemical properties of colloidal nanoparticles to their cytotoxicity. *Acc. Chem. Res.* **2013**, *46* (3), 743−749.

(18) Perez, J. M.; Asati, A.; Nath, S.; Kaittanis, C. Synthesis of biocompatible dextran-coated nanoceria with pH-dependent antioxidant properties. *Small* **2008**, *4* (5), 552−556.

(19) Alili, L.; Sack, M.; Karakoti, A. S.; Teuber, S.; Puschmann, K.; Hirst, S. M.; Reilly, C. M.; Zanger, K.; Stahl, W.; Das, S.; Seal, S.; Brenneisen, P. Combined cytotoxic and anti-invasive properties of redox-active nanoparticles in tumor−stroma interactions. *Biomaterials* **2011**, *32* (11), 2918−2929.

(20) Pelletier, D. A.; Suresh, A. K.; Holton, G. A.; McKeown, C. K.; Wang, W.; Gu, B. H.; Mortensen, N. P.; Allison, D. P.; Joy, D. C.; Allison, M. R.; Brown, S. D.; Phelps, T. J.; Doktycz, M. J. Effects of engineered cerium oxide nanoparticles on bacterial growth and viability. *Appl. Environ. Microbiol.* **2010**, *76* (24), 7981−7989.

(21) Fang, X. H.; Yu, R.; Li, B. Q.; Somasundaran, P.; Chandran, K. Stresses exerted by ZnO, CeO_2, and anatase TiO_2 nanoparticles on the *Nitrosomonas europaea*. *J. Colloid Interface Sci.* **2010**, *348* (2), 329−334.

(22) Asati, A.; Santra, S.; Kaittanis, C.; Perez, J. M. Surface-charge-dependent cell localization and cytotoxicity of cerium oxide nanoparticles. *ACS Nano* **2010**, *4* (9), 5321−5331.

(23) Kim, S. T.; Saha, K.; Kim, C.; Rotello, V. M. The role of surface functionality in determining nanoparticle cytotoxicity. *Acc. Chem. Res.* **2013**, *46* (3), 681−691.

(24) Nel, A. E.; Madler, L.; Velegol, D.; Xia, T.; Hoek, E. M. V.; Somasundaran, P.; Klaessig, F.; Castranova, V.; Thompson, M. Understanding biophysicochemical interactions at the nano-bio interface. *Nat. Mater.* **2009**, *8* (7), 543−557.

(25) Frohlich, E. The role of surface charge in cellular uptake and cytotoxicity of medical nanoparticles. *Int. J. Nanomed.* **2012**, *7*, 5577−5591.

(26) Huhn, D.; Kantner, K.; Geidel, C.; Brandholt, S.; De Cock, I.; Soenen, S. J. H.; Gil, P. R.; Montenegro, J. M.; Braeckmans, K.; Mullen, K.; Nienhaus, G. U.; Klapper, M.; Parak, W. J. Polymer-coated nanoparticles interacting with proteins and cells: Focusing on the sign of the net charge. *ACS Nano* **2013**, *7* (4), 3253−3263.

(27) Nowack, B.; Ranville, J. F.; Diamond, S.; Gallego-Urrea, J. A.; Metcalfe, C.; Rose, J.; Horne, N.; Koelmans, A. A.; Klaine, S. J. Potential scenarios for nanomaterial release and subsequent alteration in the environment. *Environ. Toxicol. Chem.* **2012**, *31* (1), 50−9.

(28) Lee, S.; Kim, K.; Shon, H.; Kim, S.; Cho, J. Biotoxicity of nanoparticles: effect of natural organic matter. *J. Nanopart. Res.* **2011**, *13* (7), 3051−3061.

(29) Lowry, G. V.; Gregory, K. B.; Apte, S. C.; Lead, J. R. Transformations of nanomaterials in the environment. *Environ. Sci. Technol.* **2012**, *46* (13), 6893−6899.

(30) Leung, M. C.; Williams, P. L.; Benedetto, A.; Au, C.; Helmcke, K. J.; Aschner, M.; Meyer, J. N. *Caenorhabditis elegans*: An emerging model in biomedical and environmental toxicology. *Toxicol. Sci.* **2008**, *106* (1), 5−28.

(31) Donkin, S. G.; Dusenbery, D. B. A soil toxicity test using the nematode *Caenorhabditis elegans* and an effective method of recovery. *Arch. Environ. Contam. Toxicol.* **1993**, *25* (2), 145−151.

(32) Handy, R. D.; Cornelis, G.; Fernandes, T.; Tsyusko, O.; Decho, A.; Sabo-Attwood, T.; Metcalfe, C.; Steevens, J. A.; Klaine, S. J.; Koelmans, A. A.; Horne, N. Ecotoxicity test methods for engineered nanomaterials: Practical experiences and recommendations from the bench. *Environ. Toxicol. Chem.* **2012**, *31* (1), 15−31.

(33) USEPA. Methods for measuring the acute toxicity of effluents and receiving waters to freshwater and marine organisms (EPA-821-R-

02−012); United States Environmental Protection Agency: Washington, DC, 2002.
(34) Donkin, S. G.; Williams, P. L. Influence of developmental stage, salts and food presence on various end-points using *Caenorhabditis elegans* for aquatic toxicity testing. *Environ. Toxicol. Chem.* **1995**, *14* (12), 2139−2147.
(35) Williams, P. L.; Dusenbery, D. B. Aquatic toxicity testing using the nematode *Caenorhabditis elegans*. *Environ. Toxicol. Chem.* **1990**, *9* (10), 1285−1290.
(36) Ravel, B.; Newville, M. ATHENA, ARTEMIS, HEPHAESTUS: Data analysis for X-ray absorption spectroscopy using IFEFFIT. *J. Synchrot. Radiat* **2005**, *12* (4), 537−541.
(37) De Faria, L. A.; Trasatti, S. The point of zero charge of CeO_2. *J. Colloid Interface Sci.* **1994**, *167* (2), 352−357.
(38) Hoecke, K. v.; Schamphelaere, K. A. C. d.; Meeren, P. v. d.; Smagghe, G.; Janssen, C. R. Aggregation and ecotoxicity of CeO_2 nanoparticles in synthetic and natural waters with variable pH, organic matter concentration and ionic strength. *Environ. Pollut.* **2011**, *159* (4), 970−976.
(39) Arnold, M. C.; Badireddy, A. R.; Wiesner, M. R.; Di Giulio, R. T.; Meyer, J. N. Cerium oxide nanoparticles are more toxic than equimolar bulk cerium oxide in *Caenorhabditis elegans*. *Arch. Environ. Contam. Toxicol.* **2013**, *65*, 224−233.
(40) Rodea-Palomares, I.; Boltes, K.; Fernandez-Pinas, F.; Leganes, F.; Garcia-Calvo, E.; Santiago, J.; Rosal, R. Physicochemical characterization and ecotoxicological assessment of CeO_2 nanoparticles using two aquatic microorganisms. *Toxicol. Sci.* **2011**, *119* (1), 135−145.
(41) Chen, K. L.; Mylon, S. E.; Elimelech, M. Aggregation kinetics of alginate-coated hematite nanoparticles in monovalent and divalent electrolytes. *Environ. Sci. Technol.* **2006**, *40* (5), 1516−1523.
(42) Liu, J. F.; Legros, S.; Von der Kammer, F.; Hofmann, T. Natural organic matter concentration and hydrochemistry influence aggregation kinetics of functionalized engineered nanoparticles. *Environ. Sci. Technol.* **2013**, *47* (9), 4113−4120.
(43) Tipping, E.; Higgins, D. C. The effect of adsorbed humic substances on the colloid stability of haematite particles. *Colloids Surf.* **1982**, *5* (2), 85−92.
(44) Bianconi, A.; Marcelli, A.; Dexpert, H.; Karnatak, R.; Kotani, A.; Jo, T.; Petiau, J. Specific intermediate-valence state of insulating 4*f* compounds detected by L_3 x-ray absorption. *Phys. Rev. B* **1987**, *35* (2), 806−812.
(45) Shahin, A. M.; Grandjean, F.; Long, G. J.; Schuman, T. P. Cerium L_{III}-Edge XAS investigation of the structure of crystalline and amorphous cerium oxides. *Chem. Mater.* **2004**, *17* (2), 315−321.
(46) Hernandez-Viezcas, J. A.; Castillo-Michel, H.; Andrews, J. C.; Cotte, M.; Rico, C.; Peralta-Videa, J. R.; Ge, Y.; Priester, J. H.; Holden, P. A.; Gardea-Torresdey, J. L. In situ synchrotron X-ray fluorescence mapping and speciation of CeO_2 and ZnO nanoparticles in soil cultivated soybean (*Glycine max*). *ACS Nano* **2013**, *7* (2), 1415−1423.
(47) Liu, W.; Rose, J.; Plantevin, S.; Auffan, M.; Bottero, J. Y.; Vidaud, C. Protein corona formation for nanomaterials and proteins of a similar size: Hard or soft corona? *Nanoscale* **2013**, *5* (4), 1658−1668.
(48) Shah, V.; Shah, S.; Shah, H.; Rispoli, F. J.; McDonnell, K. T.; Workeneh, S.; Karakoti, A.; Kumar, A.; Seal, S., Antibacterial activity of polymer coated cerium oxide nanoparticles. *Plos One* **2012**, *7*, (10).
(49) Yang, L. K.; Sundaresan, G.; Sun, M. H.; Jose, P.; Hoffman, D.; McDonagh, P. R.; Lamichhane, N.; Cutler, C. S.; Perez, J. M.; Zweit, J. Intrinsically radiolabeled multifunctional cerium oxide nanoparticles for in vivo studies. *J. Mater. Chem. B* **2013**, *1* (10), 1421−1431.
(50) Zhang, P.; Ma, Y.; Zhang, Z.; He, X.; Zhang, J.; Guo, Z.; Tai, R.; Zhao, Y.; Chai, Z. Biotransformation of ceria nanoparticles in cucumber plants. *ACS Nano* **2012**, *6* (11), 9943−9950.
(51) Perry, D. L., *Handbook of Inorganic Compounds*, 2nd ed.; CRC Press: Boca Raton, FL, 2011.
(52) Hayes, S. A.; Yu, P.; O'Keefe, T. J.; O'Keefe, M. J.; Stoffer, J. O. The phase stability of cerium species in aqueous systems: I. E-pH diagram for the Ce−$HClO_4$−H_2O system. *J. Electrochem. Soc.* **2002**, *149* (12), C623−C630.
(53) Chauhan, V. M.; Orsi, G.; Brown, A.; Pritchard, D. I.; Aylott, J. W. Mapping the pharyngeal and intestinal pH of *Caenorhabditis elegans* and real-time luminal pH oscillations using extended dynamic range pH-sensitive nanosensors. *ACS Nano* **2013**, *7* (6), 5577−5587.
(54) Cornelis, G.; Ryan, B.; McLaughlin, M. J.; Kirby, J. K.; Beak, D.; Chittleborough, D. Solubility and batch retention of CeO_2 nanoparticles in soils. *Environ. Sci. Technol.* **2011**, *45* (7), 2777−2782.
(55) Yokel, R. A.; Tseng, M. T.; Dan, M.; Unrine, J. M.; Graham, U. M.; Wu, P.; Grulke, E. A. Biodistribution and biopersistence of ceria engineered nanomaterials: Size dependence. *Nanomedicine* **2013**, *9* (3), 398−407.
(56) Go, Y. M.; Jones, D. P. Redox compartmentalization in eukaryotic cells. *Biochim. Biophys. Acta* **2008**, *1780* (11), 1273−90.
(57) Arvizo, R. R.; Miranda, O. R.; Thompson, M. A.; Pabelick, C. M.; Bhattacharya, R.; Robertson, J. D.; Rotello, V. M.; Prakash, Y. S.; Mukherjee, P. Effect of nanoparticle surface charge at the plasma membrane and beyond. *Nano Lett.* **2010**, *10* (7), 2543−2548.
(58) Tatur, S.; Maccarini, M.; Barker, R.; Nelson, A.; Fragneto, G. Effect of functionalized gold nanoparticles on floating lipid bilayers. *Langmuir* **2013**, *29* (22), 6606−6614.
(59) Moghadam, B. Y.; Hou, W. C.; Corredor, C.; Westerhoff, P.; Posner, J. D. Role of nanoparticle surface functionality in the disruption of model cell membranes. *Langmuir* **2012**, *28* (47), 16318−16326.
(60) Goodman, C. M.; McCusker, C. D.; Yilmaz, T.; Rotello, V. M. Toxicity of gold nanoparticles functionalized with cationic and anionic side chains. *Bioconjugate Chem.* **2004**, *15* (4), 897−900.
(61) Leroueil, P. R.; Berry, S. A.; Duthie, K.; Han, G.; Rotello, V. M.; McNerny, D. Q.; Baker, J. R.; Orr, B. G.; Banaszak Holl, M. M. Wide varieties of cationic nanoparticles induce defects in supported lipid bilayers. *Nano Lett.* **2008**, *8* (2), 420−424.
(62) Dobrovolskaia, M. A.; Aggarwal, P.; Hall, J. B.; McNeil, S. E. Preclinical studies to understand nanoparticle interaction with the immune system and its potential effects on nanoparticle biodistribution. *Mol. Pharm.* **2008**, *5* (4), 487−495.
(63) Arvizo, R. R.; Miranda, O. R.; Moyano, D. F.; Walden, C. A.; Giri, K.; Bhattacharya, R.; Robertson, J. D.; Rotello, V. M.; Reid, J. M.; Mukherjee, P., Modulating pharmacokinetics, tumor uptake and biodistribution by engineered nanoparticles. *Plos One* **2011**, *6*, (9).
(64) Page, A. P.; Johnstone, I. L. The cuticle. In *WormBook*; The C. elegans Research Community: **2007**.
(65) Fang-Yen, C.; Avery, L.; Samuel, A. D. T. Two size-selective mechanisms specifically trap bacteria-sized food particles in *Caenorhabditis elegans*. *Proc. Natl. Acad. Sci. U.S.A.* **2009**, *106* (47), 20093−20096.
(66) Fabrega, J.; Fawcett, S. R.; Renshaw, J. C.; Lead, J. R. Silver nanoparticle impact on bacterial growth: Effect of pH, concentration, and organic matter. *Environ. Sci. Technol.* **2009**, *43* (19), 7285−7290.
(67) Li, D.; Lyon, D. Y.; Li, Q.; Alvarez, P. J. J. Effect of soil sorption and aquatic natural organic matter on the antibacterial activity of a fullerene water suspension. *Environ. Toxicol. Chem.* **2008**, *27* (9), 1888−1894.
(68) Baalousha, M.; Le Coustumer, P.; Jones, I.; Lead, J. R. Characterisation of structural and surface speciation of representative commercially available cerium oxide nanoparticles. *Environ. Chem.* **2010**, *7* (4), 377−385.